IL NUOVO CIMENTO **46 C** (2023) 205
DOI 10.1393/ncc/i2023-23205-8

Colloquia: IPER 2022

Real-world phenomena as useful tools in physics teaching

R. De Luca([1]), O. Faella([1]) and A. Stabile([2])

([1]) *Dipartimento di Fisica "E. R. Caianiello", Università degli Studi di Salerno - 84084 Fisciano (SA), Italy*
([2]) *INFN Sezione di Napoli, Gruppo Collegato di Salerno - Salerno, Italy*

received 13 July 2023

Summary. — Delightful real-world phenomena may capture the attention of students and may trigger their curiosity. The rolling of a food can on a conveyor belt in a grocery store, the observation of the optimal angle in a shotput contest or of the way a sprinter runs, the appearance of a coloured line on a CD or a DVD under white light, the spectacular dance of sun glints on the shallow waters by the seashore are all phenomena which can be proposed to high-school or undergraduate college students in the "engagement" phase of a lecture in which the Inquiry-Based Learning approach is used. In this work we propose these examples along with a brief justification, based on elementary physics principles, of the observed phenomena.

1. – Introduction

The analysis and interpretation of real-world phenomena is the main activity of a scientist striving to contribute to the scientific progress of mankind. In the Inquiry-Based Learning (IBL) approach [1, 2] the characteristic features of the process of building up knowledge in a scientific community are used to envision a pedagogical context in which this process can be reproduced. In fact, relying on constructivism [3] and previous studies on IBL [4], the early formulation of the 5E Instructional Model, developed at the BSCS (Biological Science Curriculum Study) Centre by Bybee and co-workers [5], considers students as the true promoters of their own cultural advancement. To accomplish the ambitious goal of making students build up their own knowledge, teachers should act as facilitators and should be able to propose stimulating real-world phenomena in the "Engage" phase of the Inquiry-Based Science Education (IBSE) approach. This methodology has been proposed as one of the most promising teaching methods in science by the Rocard Commission in 2007 [6]. In the report of the Rocard Commission, however, one can detect the feeling that this approach still needs to be accepted as a common practice by teachers. In fact, it can be read [6]:

Since the origins of the declining interest among young people for science studies are found largely in the way science is taught in schools, this will be the main focus. In this context, whereas the science education community mostly agrees that pedagogical practices based on inquiry-based methods are more effective, the reality of classroom practice is that in the majority of European countries, these methods are simply not being implemented.

In this respect, real-word phenomena can give teachers some initial input in applying the IBSE instructional model. In the present work we thus propose some examples by which the curiosity of students can be captured and the "Engage" phase of an IBSE learning sequence can be designed. Observations of the proposed phenomena can be carried out by relying on their occurrence in the real world of these phenomena or by using simple experimental setups. To build up successive phases of the IBSE instructional model, namely, the Explore, the Explain, the Extend, and the Evaluate phases, a brief account of the interpretation of these phenomena is also given. In this way, also the Explain phase can be implemented by means of the mathematical treatment given in this work.

The present work is addressed to high-school or undergraduate college students and is organized as follows. In the following section, the mechanical properties of a food can rolling on a conveyor belt in a grocery store are studied. In the third section, two examples in the realm of physics of sports are proposed. In the first example, we find the optimal angle in a shotput throw by a rather simple mathematical analysis. In the second, we find the energy cost in running by an "active bouncing ball" model. In the fourth section, the appearance of a coloured line on a CD or a DVD under white light is investigated. In the fifth section, the dance of sun glints on the shallow waters by the seashore is studied. Finally, conclusive remarks are given in the last section.

2. – Physics at the grocery store

A simple physics experiment can be performed at the grocery store. Consider a cylindrical food can placed on the conveyor belt as shown in fig. 1. Assume that the conveyor belt moves, with respect to the ground, with acceleration $\vec{a}_{O'}$ along the x'-direction. Following the IBSE approach, a video taken at the grocery store of this type of motion or a demonstration in class made with common material can be part of an "Engage" phase of a physics lecture on Newton's second law when non-inertial reference

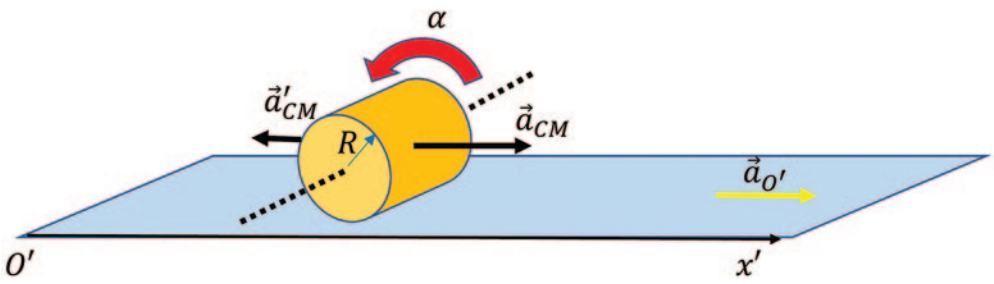

Fig. 1. – A cylinder of radius R can rotate about a longitudinal axis orthogonal to the x'-direction on a conveyor belt having acceleration $\vec{a}_{O'}$ with respect to the ground. In the reference system of the conveyor belt, the modulus of the acceleration $\vec{a}'_{CM}$ of the centre of mass can be expressed in terms of the angular acceleration α as follows: $a'_{CM} = R\alpha$. The acceleration $\vec{a}_{CM}$ can be obtained by Galilean transformations.

systems are considered. By using common material, in fact, a conveyor belt can be replaced by a sheet of paper or a cardboard which the instructor drags with his/her hands on a horizontal table. To simulate the start/stop motion of the conveyor belt, the instructor starts moving the sheet of paper from rest and puts it to stop after having pulled it for a certain distance D. By this simple experiment, students will notice that, when the phenomenon is observed in the reference system of the sheet of paper, the can rolls in such a way that its centre of mass is seen to move in a direction opposite to the positive x'-axis along which the sheet of paper slides.

We may now give a more quantitative account of this phenomenon. A more general analysis of the problem can be found in ref. [7]. In this work, we schematize the food can as a homogeneous cylinder of radius R and mass M. Because the reference frame $O'x'$ accelerates, the free rolling motion of the cylindrical body allows motion of the can's centre of mass along the x'-direction. Assuming pure rotation of this cylinder about an axis orthogonal to the x'-axis, the component of the centre of mass acceleration a'_{CM} along the x'-axis can be written as follows:

$$a'_{CM} = R\alpha, \tag{1}$$

where α is the angular acceleration of the cylindrical body. The acceleration $\vec{a}_{CM}$, as measured in the reference system of the ground, can be obtained by means of Galilean transformations, so that

$$\vec{a}_{CM} = \vec{a}'_{CM} + \vec{a}_{O'}. \tag{2}$$

So far, we have specified all kinematic quantities. We now proceed to derive the accelerations $\vec{a}'_{CM}$ and $\vec{a}_{CM}$ by Newtonian mechanics.

The forces acting on the cylinder are the following: its weight $M\vec{g}$, the normal reaction $\vec{N}$ and the friction force $\vec{F}_A$, all shown in fig. 2. In the inertial reference system of the grocery store, we may write the Newton second law as follows:

$$M\vec{g} + \vec{N} + \vec{F}_A = M\vec{a}_{CM}. \tag{3}$$

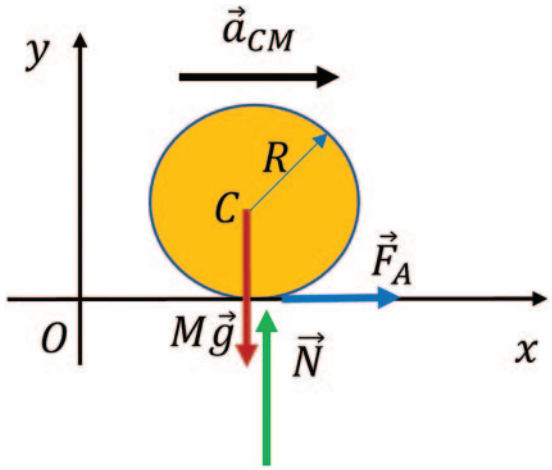

Fig. 2. – Forces acting in the homogeneous cylinder placed on an accelerating conveyor belt.

Along the x-direction, using eq. (2), we therefore have

$$F_A = M\,(-a'_{CM} + a_{O'}), \tag{4}$$

where $a'_{CM} = R\alpha$ is the modulus of the acceleration measured in the reference system of the conveyor belt as specified in eq. (1).

Furthermore, by writing the dynamical equation for the total torque $M_{ext} = F_A R$, calculated with respect to the centre of mass C of the cylinder, we may write

$$F_A R = I_{CM}\alpha, \tag{5}$$

where $I_{CM} = \frac{1}{2}MR^2$ is the moment of inertia of the cylinder. Therefore, by considering that $a'_{CM} = R\alpha$, eq. (5) can be written as follows:

$$F_A = \frac{1}{2}Ma'_{CM}. \tag{6}$$

Substituting eq. (6) into eq. (4) we obtain

$$a'_{CM} = \frac{2}{3}a_{O'}. \tag{7}$$

Therefore, the modulus of the acceleration of the centre of mass of the cylinder, as observed in the reference system of the belt, is $\vec{a}'_{CM} = -\frac{2}{3}\vec{a}_{O'}$, being it opposite to the acceleration of the belt. Therefore, by eq. (2) we have

$$\vec{a}_{CM} = \frac{1}{3}\vec{a}_{O'}. \tag{8}$$

This means that the acceleration of the centre of mass of the food can, as seen by an observer in the grocery store, is one third the acceleration of the belt.

In this way, to find the velocity $\vec{v}_{CM}$ of C, we integrate both sides of eq. (8), so that

$$\vec{v}_{CM} = \frac{1}{3}\vec{v}_{O'}, \tag{9}$$

where $\vec{v}_{O'}$ is the velocity of the conveyor belt. In eq. (9), we have made implicit the use of the initial conditions: both the conveyor belt and the can are at rest at $t = 0\,\mathrm{s}$, so that the integration constant is zero. By further integrating eq. (9) to obtain the position x_{CM} of point C on the x-axis, we have

$$x_{CM} = \frac{1}{3}x_{O'} + c, \tag{10}$$

where c is a constant and $x_{O'}$ is a position of an arbitrary point on the conveyor belt. By eq. (9), we may argue that the cashier will see the food can move toward him/her at a reduced speed with respect to the speed of the belt, the reduction factor being the same as that of the acceleration. Furthermore, from eq. (10) we may argue that the distance

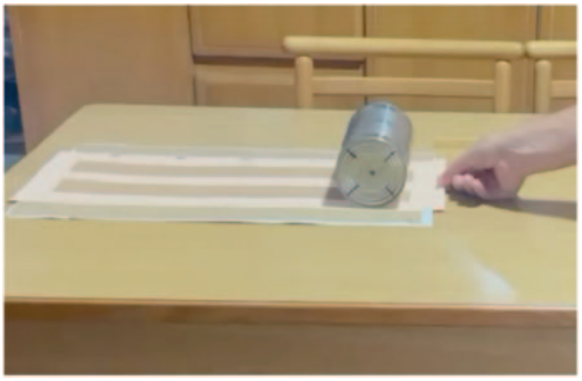

Fig. 3. – An accelerated conveyor belt can be replaced by a sheet of paper pulled from rest with acceleration $\vec{a}_{O'}$ on a table. The food can is seen to roll as specified in fig. 1 when the paper is pulled.

Δx_{CM} travelled by the food can toward the cashier in a time interval Δt, as seen by a costumer, is given by the following simple relation:

$$\Delta x_{CM} = \frac{1}{3}\Delta x_{O'}. \tag{11}$$

The cashier may feel somewhat frustrated by this reduction in the distance travelled by the can; however, this is what Newtonian mechanics is telling us, and this is what happens in the real world.

As already said before, this experiment can be reproduced by placing a homogeneous cylinder on a long sheet of paper sliding on a table, as seen in fig. 3. By this simple apparatus one can indeed see that, while the sheet of paper is pulled from rest with an acceleration $\vec{a}_{O'}$, the static initial condition of the cylinder is perturbed and it starts rolling without sliding in the way described in fig. 1, for acceleration amplitudes $a_{O'}$ lower than a threshold value $a_{O'}^{(th)}$.

It is now instructive to determine the threshold value $a_{O'}^{(th)}$ in terms of the coefficient of static friction μ_S between the can and the sheet of paper. Along the y-direction, eq. (3) reads

$$N = Mg. \tag{12}$$

On the other hand, by eq. (6) and eq. (7) we can write

$$F_A = \frac{1}{3}Ma_{O'}. \tag{13}$$

Therefore, by requiring that the can does not slip on the sheet of paper, we may set $F_A \leq \mu_S N$. By this condition, we get

$$a_{O'} \leq 3\mu_S g. \tag{14}$$

In this way, $a_{O'}^{(th)} = 3\mu_S g$. If we repeated the same analysis for a block of mass M on the accelerated sheet of paper, we would find a value of the threshold acceleration equal to $\mu_S g$. Therefore, it is easier to make a block, rather than rolling food cans, slide on a moving surface.

3. – Physics of sports

Young students are in general very much attracted by sports. Their favourite sport can ben soccer, baseball, tennis, basketball, etc. However, any other sport can attract their curiosity. In this section, we shall apply simple kinematics concepts to solve two problems. The first problem concerns the maximum range of a shotput, the second the energy cost in running.

3˙1. *Shotput kinematics.* – A simple way of describing shotput kinematics is considering the motion of a point mass launched from a point P at a height h with respect to the ground with velocity $\vec{v}_0$ at an angle θ with respect to the horizontal. The quantities h, $\vec{v}_0$, and θ are thus the relevant parameters of the problem.

Considering h and v_0 as fixed, one can ask the following question: what would be the optimum angle θ^* giving the maximum shotput range? This question has first been answered by Lichtenberg and Wills [8] by using calculus. The same problem has also been studied by other authors [9-11]. In the present analysis, we shall only use algebraic calculations to derive the same analytic formulas as in ref. [8]. Therefore, to the attractiveness of the athletic gesture related to shotput, one may add the simplicity of treating the problem only by algebraic calculations.

We start by considering the schematic representation of a shotput thrown in air by an athlete at an angle θ with respect to the horizontal as shown in fig. 4.

Therefore, by choosing the axes as in fig. 4, we may write the following equations for

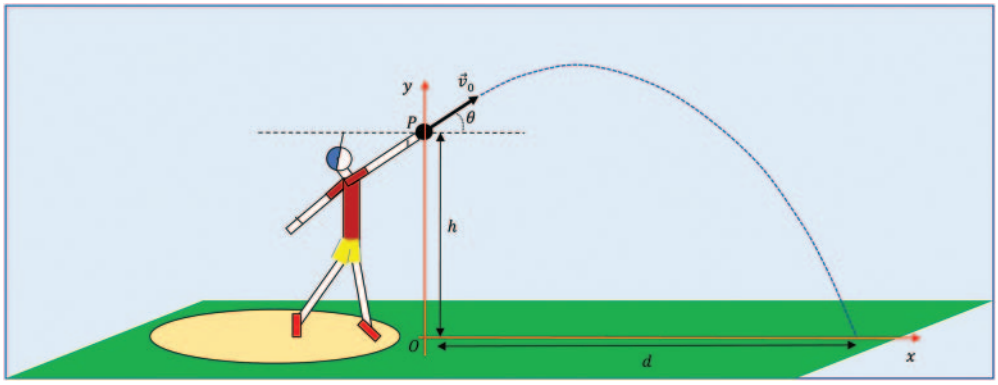

Fig. 4. – Relevant kinematic quantities in shotput: The metallic sphere is launched from P at a height h with an initial velocity $\vec{v}_0$ at an angle θ with respect to the horizontal. The shotput reaches the ground at a distance d from the origin O.

the position of the shotput as a function of time:

$$x(t) = v_0 \cos\theta t, \tag{15a}$$

$$y(t) = -\frac{1}{2}gt^2 + v_0 \sin\theta t + h. \tag{15b}$$

The trajectory $y = y(x)$ can be obtained by eliminating the parametric dependence on t from eq. (15a) by first writing $t = \frac{x}{v_0 \cos\theta}$ and by then substituting this value of t in eq. (15b), so that

$$y(x) = h + \tan\theta x - \frac{g}{2v_0^2 \cos^2\theta}x^2. \tag{16}$$

Setting $y(d) = 0$ in eq. (16), we may obtain the angle θ at which the shotput was launched in air. In fact, by further writing $\frac{1}{\cos^2\theta} = 1 + \tan^2\theta$, and by defining $\eta = \tan\theta$, we may express the condition $y(d) = 0$ as follows:

$$\eta^2 - \frac{2v_0^2}{gd}\eta + 1 - \frac{2v_0^2 h}{gd^2} = 0. \tag{17}$$

A positive real solution to the above second-degree algebraic equation can be found only if the discriminant Δ is greater or equal to zero. In this way, we set

$$\left(\frac{2v_0^2}{gd}\right)^2 - 4\left(1 - \frac{2v_0^2 h}{gd^2}\right) \geq 0. \tag{18}$$

By simple algebraic calculations, we may thus write the above relation as follows:

$$d \leq \frac{v_0\sqrt{v_0^2 + 2gh}}{g}. \tag{19}$$

Here we realize that the quantity $v_1 = \sqrt{v_0^2 + 2gh}$ is the speed of the shotput when it reaches the ground. eq. (19) thus tells us that, for given values of v_0 and h, the shotput cannot go beyond the distance $d = R = \frac{v_0\sqrt{v_0^2+2gh}}{g}$. In this way, the maximum shotput range is the following:

$$R = \frac{v_0 v_1}{g}. \tag{20}$$

The above expression, written in this form, provides the optimal angle in a rather concise form. In fact, by noticing that the solution η^* to eq. (17), for $\Delta = 0$, can be written as $\frac{v_0^2}{gR}$, by means of eq. (20), we have:

$$\eta^* = \tan\theta^* = \frac{v_0}{v_1}. \tag{21}$$

This relation is equally simple. By recalling that $\eta = \tan\theta$, we notice that the optimal angle $\theta^* = \tan^{-1}\left(\frac{v_0}{v_1}\right)$ is less than $45°$ since $0 < \frac{v_0}{v_1} < 1$. The rather simple gesture in the shotput discipline thus allows us to discuss, in a more general way, the kinematics of

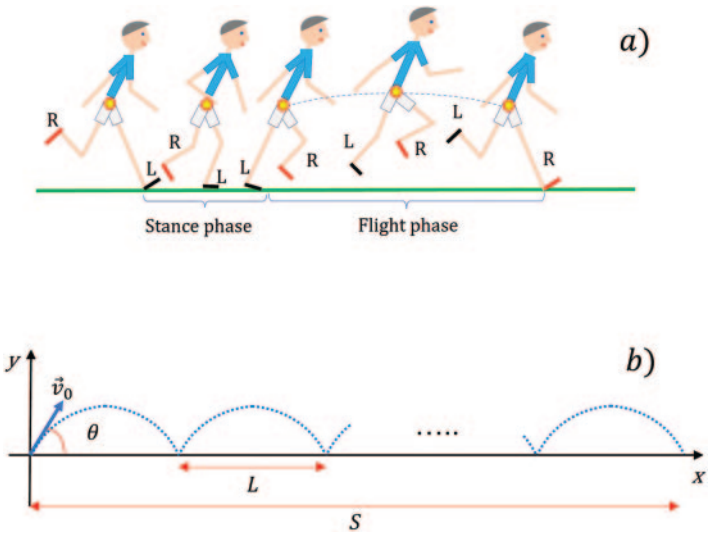

Fig. 5. – (a) Schematic representation of the stance and flight phases in a single step during running. In the stance phase, one foot (L in this figure) is in contact with the ground. During the flight phase, both feet and the whole body are suspended in air. Here the length of a step can be defined as the distance from the touch-down point of one foot (L) to the touch-down point of the contralateral foot (R). (b) Motion of Centre of Mass (CoM) during horizontal running. Considering the stance phase instantaneous, the CoM, shown as a yellow point, just touches the x-axis in all points connecting adjacent parabolas.

a point particle launched from a height h. It is instructive to let students calculate the value of θ^* and R for $h = 0$. Students will soon recognize the usual results for projectile motion briefly recalled in the following section.

3˙2. *Energy cost in running.* – A second useful example in discussing physics of sports is the schematic representation of the flight phase in running shown in fig. 5(a). By this simplified description of the running activity and by the application of simple concepts in classical physics one can determine the energy cost for a given person moving on a horizontal plane. This problem has been proposed to high-school students in the 2023 "*Premio Caianiello*" contest, which takes place year at the Physics Department of Salerno University (ITALY). A more detailed treatment of this same problem can be found in ref. [12].

The motion of an athlete of mass m during running can be studied by neglecting air resistance and by considering the stance phase, when one foot is in contact with the ground, as instantaneous [12]. Under these conditions, the Centre of Mass (CoM) of the athlete (yellow point in fig. 5(a)) follows a parabolic trajectory at each step. Accordingly, the CoM behaves as a bouncing ball whose complete approximate trajectory is given by a sequence of identical parabolas, as shown in fig. 5(b). By this simple model, one can calculate the total energy spent by this athlete to run over the distance S.

The analytic expression of the length $L(\theta)$ of each step of the athlete, *i.e.*, the distance from the take-off point to the next landing point, can be found in terms of the amplitude v_0 of the initial velocity of the flight phase, of the acceleration due to gravity g, and of the angle θ (see first parabola in fig. 5(b)). By using the results of a projectile motion [13],

when the projectile is launched from the same height at which it lands, we may write

$$L(\theta) = \frac{v_0^2}{g}\sin(2\theta). \tag{22}$$

We now introduce the coefficient of restitution ε for each bounce [13], so that $\varepsilon = \frac{v_1}{v_0}$, where v_0 is the speed of the athlete's CoM immediately before impact with the ground and v_1 would be the CoM take-off velocity if no work input from the limb muscles compensated for the mechanical energy loss ΔE during the anelastic collision of the instantaneous stance. The muscle action is thus able to restore the initial velocity v_0, so that the energy cost at each step is given by the following expression:

$$\Delta E = \frac{1}{2}m\left(v_0^2 - v_1^2\right) = \left(1-\varepsilon^2\right)\frac{1}{2}mv_0^2. \tag{23}$$

We may now define the total mechanical energy dissipated over the distance S as $E_{TOT}(\theta) = N\Delta E$, where $N = \frac{S}{L}$ is the total number of steps taken by the athlete to go through the distance S. In this way, by recalling eq. (23), we have

$$E_{TOT}(\theta) = \frac{1}{2}\frac{\left(1-\varepsilon^2\right)}{\sin(2\theta)}mgS. \tag{24}$$

The minimum value E_{min} of the above quantity is obtained for $\theta = \frac{\pi}{4}$, so that

$$E_{min} = \frac{1}{2}\left(1-\varepsilon^2\right)mgS. \tag{25}$$

Define now the quantity $k = \frac{E_{TOT}(\theta)}{mS} \geq \frac{E_{min}}{mS}$. When $S = 1.00\,\mathrm{km}$, this quantity defines the mechanical energy cost for a run of 1.00 km for each kilogram of mass of the athlete, so that we may measure it in $\frac{\mathrm{kJ}}{\mathrm{kg\,km}}$. In this way, we have

$$k \geq \frac{1}{2}\left(1-\varepsilon^2\right)g. \tag{26}$$

Considering that the human body has an efficiency of about 25% in converting chemical energy into mechanical energy, we may define the chemical energy necessary to run over one kilometre per each kilogram of mass of the athlete K as four times the value of k, so that

$$K \geq 2\left(1-\varepsilon^2\right)g. \tag{27}$$

Under the hypotheses made above, the coefficient of restitution ε can be estimated by comparing the expression for the quantity K in eq. (27) with the experimentally determined value of about $4.2\frac{\mathrm{kJ}}{\mathrm{kg\cdot km}}$ [14, 15] for the metabolic energy cost. In this way, by setting $K_{min} = 2\left(1-\varepsilon^2\right)g = K_{exp} = 4.2\frac{\mathrm{kJ}}{\mathrm{kg\cdot km}}$, one finds $\varepsilon = 0.89$. By finally converting the value of K_{exp} in kcals, we may see that

$$K_{exp} \approx 1.0\frac{\mathrm{kcal}}{\mathrm{kg}\cdot\mathrm{km}}. \tag{28}$$

Therefore, an athlete of mass 75.0 kg running for a kilometre spends, on the average, about 75 kcal.

The above analysis can be useful to show how simple concepts in kinematics may be used to derive physical constants which allow students to calculate, for example, energy expenditure during a jogging session. Students will thus be aware that the kinematics concepts learned in class can be useful in a rather diffused discipline as running. They may also obtain videos of them running with a visible point attached to their body as in fig. 5(a) and make successive video analysis to prove the validity of the "active bouncing ball" model.

4. – Coloured lines on CDs or DVDs under white light

In 2015, during the international year of light, the characteristic features arising from a CD held horizontally under a lamp have been used in the Summer School of Physics at University of Salerno. This Summer School is dedicated to advanced high-school students and is held yearly at the Physics Department in Salerno. The analysis of this simply reproducible phenomenon provides a quite simple way of introducing the effects of interference and diffraction in optical systems to students. Let us now see what happens when a CD or a DVD is held under skimming light rays from a lamp, as shown in fig. 6. As done in ref. [16], we first ask the question: Why do we see a (coloured) line? Successively, one might consider what colour can be seen when looking at a CD or at a DVD. Some students at the Summer School had already noticed this phenomenon by themselves and others were already capable to distinguish a CD from a DVD by this simple experiment.

The reason why we see a line is due to the law of reflection [16]. Refer to fig. 7 and consider an observer in O and a light source in S, both placed on the same horizontal plane. The light source sends skimming light rays to a CD or a DVD. These light rays are incident on the tracks of these devices and are reflected as shown in fig. 7. However, only when light rays are incident on the line bisecting the segment OS shown in fig. 7, at points P and P', for example, the observer can see the reflected ray. In all other cases (see reflection of the light ray in P'' in fig. 7, for instance) the same is not true. In fact, the light ray incident at point P'' is reflected in a direction away from the observer. Therefore, the observer sees a line on the device along a direction between

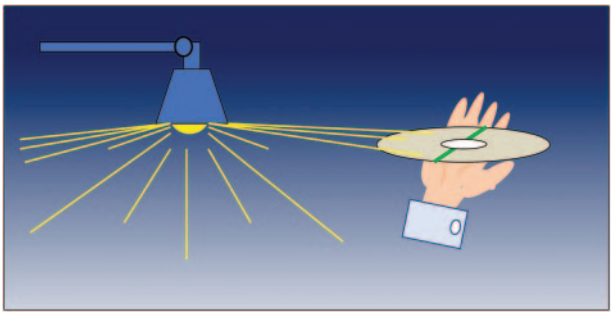

Fig. 6. – By holding a CD horizontally in one hand and by letting skimming light rays from a lamp fall on the device, one is able to see a green line. When a DVD is used, the line has a cyan color.

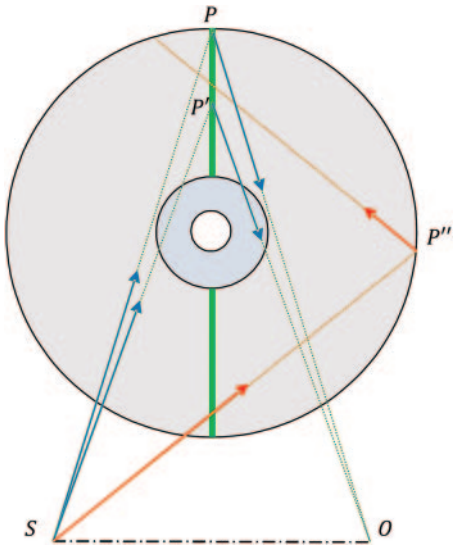

Fig. 7. – Light rays from S are incident on the tracks of a CD. An observer is placed in O. Only those rays that are incident on the line bisecting the segment SO on the CD, as those incident in P and P', can been seen by the observer. As an example, the light ray incident in P'' cannot reach point O.

his/her position and the position of the lamp.

The reason why one sees a line of a given colour is because CDs and DVDs behave as diffraction gratings. To give a plausible explanation of this fact, one can proceed as in ref. [16]. Referring to fig. 8, consider a generic point P on the coloured upper segment lying along the bisecting line passing through HC. By letting d represent the length of the segment HC and by taking the radius of the region of the CD not covered by tracks

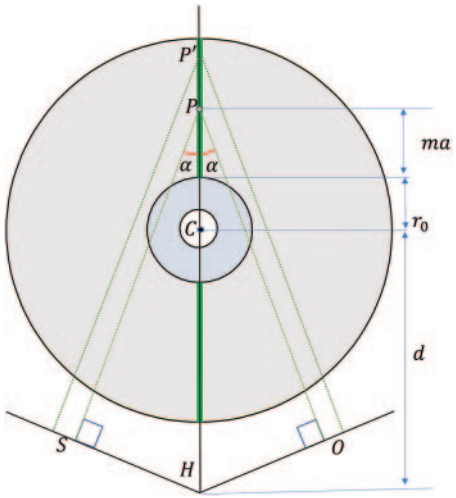

Fig. 8. – Geometric quantities related to the propagation of parallel light rays from the source S to the position O of the observer.

to be r_0, the length r of the path followed by a wavelet originated in S from S to O is [17]:

$$r = 2\,(d + r_0 + ma)\cos\alpha, \tag{29}$$

where m is an integer defining the number of tracks, a is the pitch, and α is the angle between the direction of propagation of the wavelet and the coloured line. Therefore, in the approximation of scalar diffraction theory [18], the observer at O will see reflected wavelets at a frequency $\nu = \frac{c}{\lambda} = \frac{ck}{2\pi}$ from each track characterized by the following expression of the electric field:

$$\vec{E}_m = \vec{E}_0 e^{i2k(d+r_0+ma)\cos\alpha} = \vec{E}_0 e^{i2k(d+r_0)\cos\alpha}\left(e^{2ika\cos\alpha}\right)^m, \tag{30}$$

where, as usual, only the real part of $\vec{E}_m$ is considered. Here we notice that the electric field is seen as a plane wave and that its mathematical expression in terms of complex number is very convenient, for what we shall see next. In fact, by summing from $m = 0$ to N, where N is the total number of tracks, we may write the total electric field as follows:

$$\vec{E} = \sum_{m=0}^{N} \vec{E}_m = \vec{E}_0 e^{i2k(d+r_0)\cos\alpha} \sum_{m=0}^{N} \left(e^{2ika\cos\alpha}\right)^m. \tag{31}$$

By noticing that the partial sum $S_N = \sum_{m=0}^{N} s^m = 1 + s + s^2 + \ldots + s^N$ is equal to $S_N = \frac{s^{N+1}-1}{s-1}$, eq. (31) can be written as follows:

$$\vec{E} = \vec{E}_0 e^{i2\tilde{k}(d+r_0)} \frac{\left(e^{i2\tilde{k}a}\right)^{N+1} - 1}{\left(e^{i2\tilde{k}a}\right) - 1}, \tag{32}$$

where $\tilde{k} = k\cos\alpha$. One may now write eq. (32) in the following form:

$$\vec{E} = \vec{E}_0 e^{i2\tilde{k}(d+r_0)} e^{\left(iN\tilde{k}a\right)} \frac{\sin\left[(N+1\tilde{k}a\right]}{\sin\left(\tilde{k}a\right)}. \tag{33}$$

Since the light intensity I at O is proportional to $\left|\vec{E}\right|^2$ [18], the complex phase factors disappear in the expression for I, so that

$$I = I_0 \frac{\sin^2\left[\frac{(N+1)}{2}\tilde{k}a\right]}{\sin^2\left(\frac{\tilde{k}a}{2}\right)}. \tag{34}$$

By now recalling that $\tilde{k} = k\cos\alpha = \frac{2\pi}{\lambda}\cos\alpha$, where λ is the wavelength of the radiation in the visible spectrum, eq. (34) can be written as follows:

$$I = I_0 \frac{\sin^2\left[\frac{2(N+1)\pi a}{\lambda}\cos\alpha\right]}{\sin^2\left(\frac{2\pi a}{\lambda}\cos\alpha\right)}. \tag{35}$$

The above equation closely recalls the pattern of a diffraction grating. The maxima of these curves are located at values of the quantity $\frac{2a}{\lambda}\cos\alpha = M$, where M is an integer, so that

$$\lambda_M = \frac{2a}{M}\cos\alpha. \tag{36}$$

For $\cos\alpha \approx 1$ (small values of the angle α), this expression reduces to $\lambda_M \approx \frac{2a}{M}$. This expression is mathematically accessible and can now be used for very simple calculations.

For a CD, one sets $a = 1600\,\text{nm}$. By requiring that $400\,\text{nm} < \lambda_M < 700\,\text{nm}$, assuming $\cos\alpha \approx 1$ in eq. (36), one may find that this inequality is satisfied for the following values of the integer *M:* 5,6,7,8. Corresponding to these values of M we have

$$\lambda_5 = 640\,\text{nm}; \quad \lambda_6 = 533\,\text{nm}; \quad \lambda_7 = 457\,\text{nm}; \quad \lambda_8 = 400\,\text{nm}. \tag{37}$$

Apart from the peripheral value $\lambda_8 = 400\,\text{nm}$, the closest value to the maximum eye sensitivity region is $\lambda_6 = 533\,\text{nm}$, which corresponds to the green portion of the visible light spectrum. Other wavelengths $\lambda_5 = 640\,\text{nm}$ (red) and $\lambda_7 = 457\,\text{nm}$ (blue) should however be detected in spectrographic measurements.

For a DVD one sets $a = 740\,\text{nm}$. By requiring again that $400\,\text{nm} < \lambda_M < 700\,\text{nm}$, assuming $\cos\alpha \approx 1$ in eq. (36), one sees that the previous inequality is satisfied only for $M = 3$. Corresponding to this value of M, one has [17]:

$$\lambda_3 = 493\,\text{nm}. \tag{38}$$

The wavelength λ_3 falls within the cyan portion of the visible spectrum.

Therefore, if one needs to distinguish a CD from a DVD, one only needs to check the colour of the line seen under skimming light rays. If the line is green, the device is a CD; on the other hand, if the line is cyan, the device is a DVD. In an "Extend" phase, the same type of reasoning could be repeated in the case of a "blue ray" device, whose pitch is $a = 320\,\text{nm}$. These types of devices (CDs, DVDs or "blue ray") are commonly available. Their presence in a physics classroom may represent a good chance to improve the competence in optics of our physics students.

5. – Sun glints by the seashore

When looking at the shallow calm water of the sea in a sunny summer day, one might notice the appearance of sun glints in the proximity of the beachfront. The spectacular dance of these glints is the result of reflection of light from the slowly undulating sea water. This phenomenon, reported in fig. 9 and studied in detail in ref. [19], may be used to introduce Fresnel equations.

We may first introduce the conditions by which Fresnel equations are derived. Therefore, by considering either the case in which the electric field is in a direction parallel to the incidence plane as shown in fig. 10(a) or the case in which the electric field is in a direction orthogonal to the incidence plane as in fig. 10(b), the reflection and transmission coefficients, R and T, respectively, can be derived by imposing the interface conditions on the component of the electric field and the fields parallel and orthogonal to the surface.

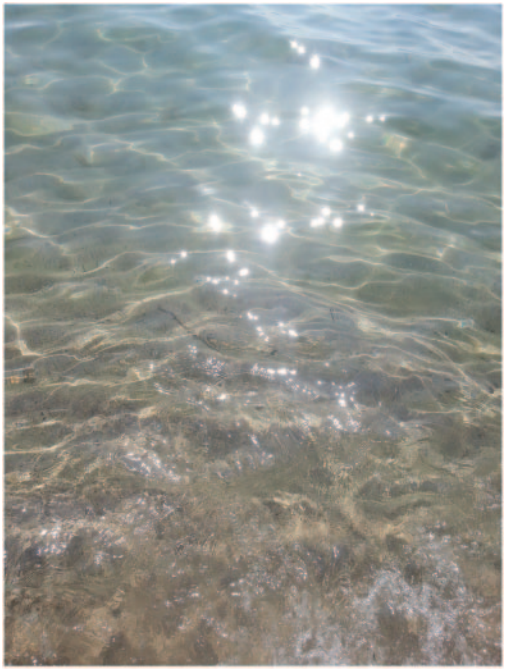

Fig. 9. – Sun glints near the beachfront. The star-like glints gently dance on the undulating sea water.

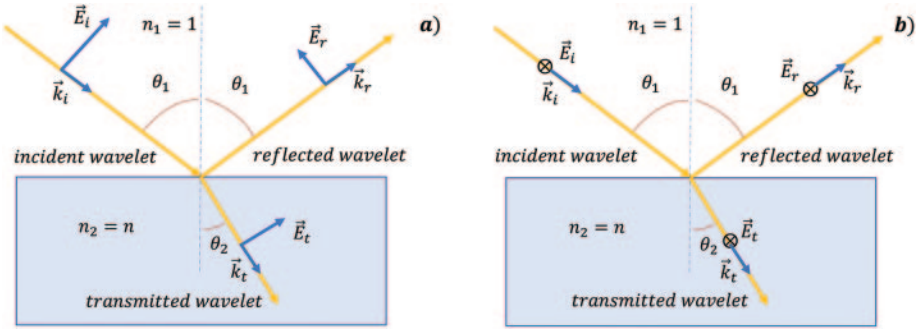

Fig. 10. – Reflection and refraction of light coming from air with index of refraction $n_1 = 1$ and incident on a smooth surface of a transparent medium with index of refraction $n_2 = n$. In panel (a), the electric field is polarized parallel to the incidence plane, in panel (b), the electric field is orthogonal to the incidence plane.

In the first case , we obtain the coefficients R_p and T_p for p-polarized light, which are given by the following expressions:

$$R_p = \left(\frac{n \cos\theta_1 - \cos\theta_2}{n \cos\theta_1 + \cos\theta_2} \right)^2, \quad T_p = 1 - R_p, \tag{39}$$

where θ_1 and θ_2 are the incidence and refracted angle, respectively, both comprised

between 0 and $\frac{\pi}{2}$, and n is the index of refraction of sea water.

By Snell's law [19], we can now express the term $\cos\theta_2$ in terms of the incidence angle θ_1 as follows:

$$\cos\theta_2 = \sqrt{1 - \frac{\sin^2\theta_1}{n^2}}, \tag{40}$$

so that eq. 40) becomes

$$R_p = \left[\frac{n\cos\theta_1 - \sqrt{1 - \frac{\sin^2\theta_1}{n^2}}}{n\cos\theta_1 + \sqrt{1 - \frac{\sin^2\theta_1}{n^2}}}\right]^2. \tag{41}$$

As it is well known, by this expression one can derive the expression for the Brewster angle $\theta_B = \tan^{-1} n$, giving a null value of R_p.

On the other hand, the reflectance and transmittance of s-polarized light are given by the following:

$$R_s = \left(\frac{\cos\theta_1 - n\cos\theta_2}{\cos\theta_1 + n\cos\theta_2}\right)^2, \quad T_s = 1 - R_s. \tag{42}$$

Therefore, because of eq. (40), the reflectance R_s will have the following form:

$$R_s = \left[\frac{\cos\theta_1 - n\sqrt{1 - \frac{\sin^2\theta_1}{n^2}}}{\cos\theta_1 + n\sqrt{1 - \frac{\sin^2\theta_1}{n^2}}}\right]^2. \tag{43}$$

It is also well-known that the above expression is not equal to zero for any value for the angle θ_1, as it can also be proven by direct calculation.

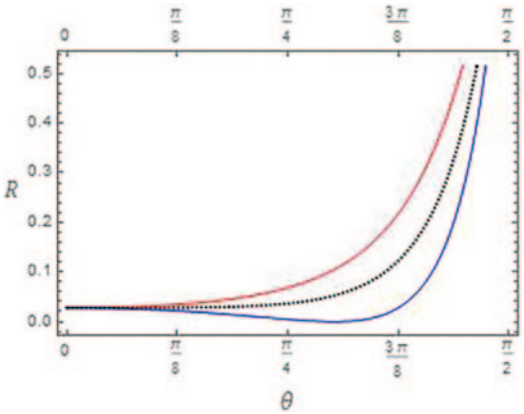

Fig. 11. – Reflectance of sea water under p-polarized light (blue curve), s-polarized light (red curve), and unpolarized light (dotted black curve).

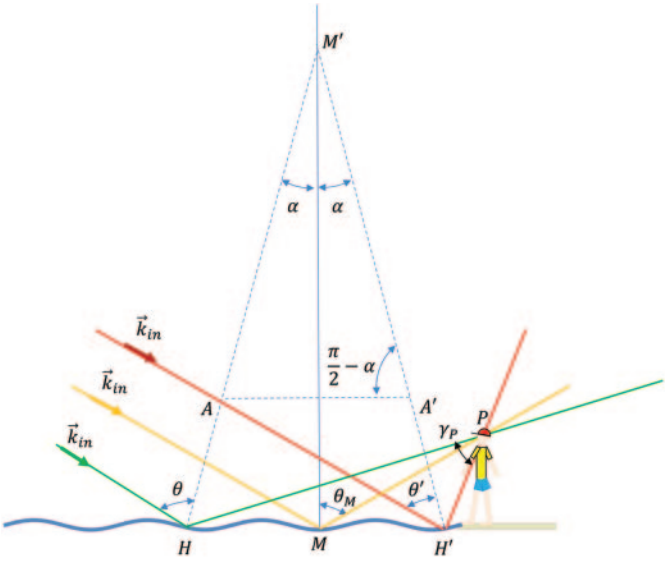

Fig. 12. – In order to determine the angular length γ_P of the glitter pattern on sea water, one needs to schematize reflection of parallel wavelets (red, yellow, and green) by the waves and consider only those which an observer in P can see. All visible wavelets in P are comprised between the direction of the red and green segments HP and $H'P$.

Finally, for non-polarized light, we may write the reflectance R as follows:

$$R = \frac{R_p + R_s}{2}. \tag{44}$$

The reflectance of sea water ($n = 1.4$) under p-polarized, s-polarized and unpolarized light is shown in fig. 11. In this figure we notice that the Brewster angle ($\theta_B = 54.5°$ for sea water) is comprised between $\frac{\pi}{4}$ and $\frac{3\pi}{8}$. We might also notice that the reflectance of sea water for unpolarized light is an increasing function of θ_1. Having reviewed these well-known aspects concerning the reflection of light by a transparent medium, we now turn our attention to reflection of sunlight on slowly undulating waves.

Let us first consider the conditions by which sun glints may be seen by an observer on the seashore. We thus calculate the angular length γ_P of the glitter pattern following the schematic representation of light reflection represented in fig. 12. Being the Sun at very great distances from Earth, we assume that the propagation vectors $\vec{k}_{in}$ of the incident wavelets are parallel. Three incident wavelets on the sea water are shown in fig. 12: one red, one yellow, and one green. The red wavelet is incident in point H', close to the observer in P, at an angle θ' with respect to the normal to the wave surface. The yellow wavelet is incident in M at an angle θ_M with respect to the local normal, corresponding to the zenith. Finally, the green wavelet is incident in point H, farther from the observer, at an angle θ with respect to the normal to the wave surface. The local normal in H and H' is inclined of a minimum value $-\alpha$ and a maximum value $+\alpha$ with respect to the zenith, respectively. In this way, these lines intersect in M, as shown in fig. 12. By now considering the triangle $\widehat{\mathbf{AM'H'}}$ and by summing the internal angles, one obtains

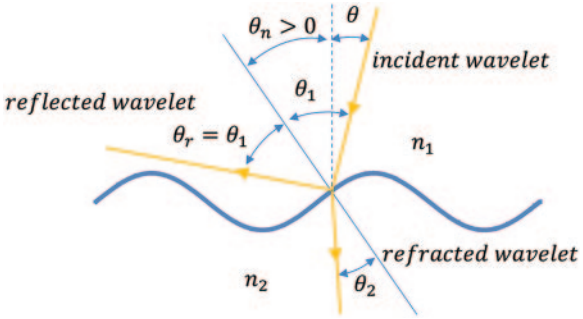

Fig. 13. – A light wavelet incident on sea water. The incidence angle θ_1 can be expressed as the sum between the angular displacement θ of the position of the Sun with respect to the zenith and the angle θ_n between the normal to the point of incidence and the zenith.

the following expression:

$$2\alpha = \theta - \theta'. \tag{45}$$

On the other hand, by summing the internal angles of the triangle $\widehat{PHH'}$, one gets

$$\gamma_P = 2\alpha + \theta - \theta'. \tag{46}$$

Considering eqs. (45) and (46), the following simple relation for γ_P in terms of the angle α can be derived:

$$\gamma_P = 4\alpha. \tag{47}$$

Therefore, the angular length of the glitter pattern for calm sea water (small values of α) is not too broad, as it can be argued from fig. 9.

To detect the points in which the maximum value of the reflectance occurs, one can schematize a sea wave as in fig. 13. The sea wave can then be mathematically represented by a sinusoidal function $w(x)$ of the following type:

$$w(x) = a\left[1 + \sin\left(\frac{2\pi}{\lambda}x\right)\right], \tag{48}$$

where λ is the wavelength of the sea wave and where x is the distance from the beach front. The expression in eq. (48) is rather simple; nevertheless, it allows us to grasp some characteristic features of the phenomenon of sun glints in calm sea water.

From fig. 13 we can notice that the incidence angle θ_1 can be expressed as the sum of the angular displacement θ of the Sun with respect to the zenith and of the angle θ_n between the normal to the point of incidence and the zenith, so that

$$\theta_1 = \theta + \theta_n. \tag{49}$$

Therefore, the angle θ_n represents the angle by which the tangent to the curve $w(x)$ is inclined with respect to the horizontal. In this way, by the definition of derivative, we

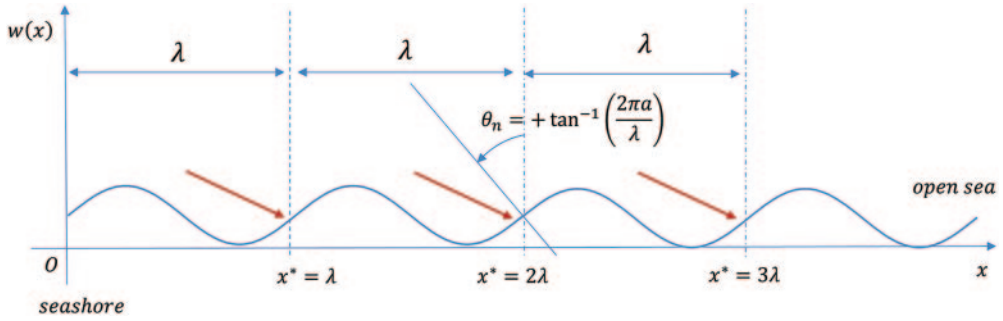

Fig. 14. – A sea-wave is described by means of the sinusoidal function $w(x) = a\left[1 + \sin\left(\frac{2\pi}{\lambda}x\right)\right]$. The points in which maximum reflectance is obtained are those obeying the relation $x^* = n\lambda$, where $x = x^*$ is the distance of these points from the seafront.

have $w'(x) = \tan\theta_n$, so that, by taking the derivative of $w(x)$ in eq. (48), we may write:

$$\tan\theta_n = \frac{2\pi a}{\lambda}\cos\left(\frac{2\pi}{\lambda}x\right), \tag{50}$$

so that

$$\theta_n(x) = \tan^{-1}\left[\frac{2\pi a}{\lambda}\cos\left(\frac{2\pi}{\lambda}x\right)\right]. \tag{51}$$

We have noticed before that the reflectance R is an increasing function of θ_1. By then considering the angle θ as fixed at a certain hour of the day, we can look for the points of maximum reflectance on the wave by considering that θ_n varies in the interval $\left[-\tan^{-1}\left[\frac{2\pi a}{\lambda}\right], +\tan^{-1}\left[\frac{2\pi a}{\lambda}\right]\right]$. Therefore, the maximum values of R is obtained for $\theta_n(x^*) = +\tan^{-1}\left[\frac{2\pi a}{\lambda}\right]$, *i.e.*, for $\cos\left(\frac{2\pi}{\lambda}x^*\right) = 1$. In this way, at the following value of the distance x^*:

$$x^* = n\lambda, \tag{52}$$

where n is a nonnegative integer. These points are shown in fig. 14.

Naturally, only those luminous spots which are close to the maximum reflectance points shown in fig. 14 and which lie within the angular length γ_P of the glitter pattern given in eq. (47) will be visible by an observer on the seashore in O. As for the expression of γ_P, we may notice that, given the mathematical expression of the wave in eq. (48), by setting $\alpha = \theta_n(x^*) = +\tan^{-1}\left[\frac{2\pi a}{\lambda}\right]$, we may write

$$\gamma_P = 4\tan^{-1}\left[\frac{2\pi a}{\lambda}\right]. \tag{53}$$

In fact, if the local normal of the wave is inclined of an angle α with respect to the zenith, the tangent to the curve has the same inclination with respect to the horizontal.

For calm water, setting $a \approx 1.0\,\text{cm}$ and $\lambda \approx 20\,\text{cm}$, we have that the angular length of the phenomenon is $\gamma_P \approx 70°$. To estimate the extension L of the pattern for an observer

of height h, referring to fig. 12, we may set $\frac{L}{h} \approx \tan\gamma_P$. In this way, for $\gamma_P \approx 70^\circ$ and for an average observer of height $h \approx 1.7\,\mathrm{m}$, we have $L \approx 4.7\,\mathrm{m}$.

Naturally, it is not possible to make experiments on this phenomenon on the beach. However, a physics teacher might film the sun glints and record the angular position of the Sun with respect to the zenith at the same moment. An approximate evaluation of the angular length of the glint pattern could also be obtained by direct measurements. By roughly estimating the quantities a and λ, finally, the relation in eq. (53) can be verified.

6. – Conclusions

During our teaching experience at high-school or undergraduate level, we have been able to notice that students are much attracted by real-world phenomena. Some of these occurrences capture their attention and give them the right motivation to learn about possible explanations based on underlying simple physics concepts. In this way, we have been able to gather few examples in which these real-world phenomena can be readily brought to the attention of high-school or university students. In this respect, these examples can be considered to be "useful tools in physics teaching". Naturally, our experience can only confirm validity of the Inquiry-Based Learning approach [1, 2]. We therefore propose these same examples as part of the "Engage" and "Explain" phases of a teaching unit designed according to the 5E Instructional Model [5].

The simplest examples proposed in the present work are represented by the rolling of a food can on a conveyor belt in a grocery store and by the way the optimal angle in a shotput can be found. A more complex model, though still treated with basic kinematics, is the "active bouncing ball" description of running. The appearance of a coloured line in a CD or a DVD held horizontally in front of us under the light of a lamp provides a clear example of how the undulatory theory of optics can be applied to explain why a green line is visible on a CD and why this line is blue on a DVD. These findings were used during the 2015 edition (international year of light) of the Summer School in Physics, held yearly at University of Salerno. The wonderful dance of sun glints appearing by the seashore on calm water in a warm sunny day on the beach can finally give a taste to young students of how the mind of a physicist works and how scientific progress is brought about. In fact, even after having observed an apparently simple phenomena occurring in nature, like the sun glints near the seashore, a physicist asks himself/herself what the right mathematical and logical instruments to explain what he/she sees might be. He/she then tries to interpret, on the basis of these instruments, the observed phenomenon. Having provided his/her interpretation, the scientific community validates or refutes the explanation given. Possibly, other scientists elaborate further what is observed and explained by the single researcher. In this way, students may argue that the process of building up scientific knowledge is rather similar to the phases described in the 5E Instructional Model.

REFERENCES

[1] Atkin J. M. and Karplus R., *Sci. Teach.*, **29** (1962) 45.
[2] Barrow L., *J. Sci. Educ.*, **17** (2006) 265.
[3] Piaget J., *Behaviour and Evolution* (Routledge, London) 1979.
[4] Bruner J., *The Process of Education* (Harvard University Press, Cambridge, MA) 1960.
[5] Bybee R. W. and Landes N. M., *Am. Biol. Teach.*, **52** (1990) 92.

[6] https://www.eesc.europa.eu/sites/default/files/resources/docs/rapportrocardfinal.pdf.
[7] De Luca R., *Rev. Bras. Ensino Fis.*, **44** (2020) e20220086.
[8] Lichtenberg D. B. and Wills J. G., *Am. J. Phys.*, **46** (1978) 546.
[9] Baće M., Ilijić S. and Natančić Z., *Eur. J. Phys.*, **23** (2002) 409.
[10] De Luca R., *Eur. J. Phys.*, **26** (2005) 1031.
[11] Gangi S. and Lagormasino D., *Eur. J. Phys.*, **35** (2014) 045026.
[12] Borgongino L., Rufrano Aliberti S., Romeo F. and De Luca R., *Eur. J. Phys.*, **43** (2022) 015802.
[13] Sears F. W., Zemansky M. W. and Young H. D., *University Physics*, 5th edition (Addison-Wesley, Reading) 1977.
[14] Margaria R., Cerretelli P., Aghemo P. and Sassi G., *J. Appl. Physiol.*, **18** (1963) 367.
[15] Minetti A. E., Gaudino P., Seminati E. and Cazzola D., *J. Appl. Physiol.*, **144** (2013) 498.
[16] De Luca R., Di Mauro M., Fiore O. and Naddeo A., *Am. J. Phys.*, **86** (2018) 169.
[17] De Luca R., Di Mauro M., Fiore O. and Naddeo A., *Am. J. Phys.*, **91** (2023) 487.
[18] Goodman J. W., *Introduction to Fourier Optics* (Roberts and Company Publishers, Greenwood Village, New York) 2005.
[19] Halliday D., Resnick R. and Walker J., *Fundamentals of Physics*, 7th edition (Wiley and Sons, New York) 2005.